

Observation of Kerr nonlinearity and Kerr-like nonlinearity induced by terahertz generation in LiNbO₃

Bo Wang,^{1,2} Chun Wang,^{1,2} Li Wang,¹ and Xiaojun Wu^{3, a)}

¹⁾Beijing National Laboratory for Condensed Matter Physics, Institute of Physics, Chinese Academy of Sciences, Beijing 100190, China

²⁾School of Physical Sciences, University of Chinese Academy of Sciences, Beijing 100049, China

³⁾Beijing Key Laboratory for Microwave Sensing and Security Applications, School of Electronic and Information Engineering, Beihang University, Beijing, 100083, China

(Dated: 18 March 2022)

Femtosecond laser pulses interacting with LiNbO₃ has been widely applied in intense terahertz generation, excitation and imaging of phonon polaritons and modulating light. It is of great importance to study the nonlinearities induced by femtosecond laser pulses in LiNbO₃. Here, we demonstrate that both Kerr nonlinearity and Kerr-like nonlinearity induced by terahertz wave occur under the interaction between laser pulses and LiNbO₃ using optical pump-probe techniques. We show that the contribution of Kerr-like nonlinearity to pump-probe spectra varies with the interaction length because of the phase mismatching between terahertz wave and laser pulse. We also observed the excitation of the low frequency phonon polaritons. Experimental results are in consistent with theoretical calculation.

Since the invention of laser, nonlinear optics has always been drawing attentions of researchers. LiNbO₃ is one of the most important nonlinear optical crystals¹ with applications in waveguides² and high speed modulators³. Especially in terahertz (THz) science and technology, LiNbO₃ is widely used in intense THz sources^{4,5} under the illumination of femtosecond laser pulses with the tilted pulse front technique. Femtosecond laser pulses induced nonlinearity in LiNbO₃ is of great significance to study.

In recent decades, one of interests in LiNbO₃ is excitation and detection of phonon polaritons with pump-probe techniques in which one or two femtosecond laser beams excite phonon polaritons and a weaker probe beam detects the refractive index changes caused by them⁶. However, the induction of coherent phonon polaritons is not the only nonlinear optical effect when femtosecond laser pulses interact with electro-optic crystals. Third order optical nonlinearity exists in media with any symmetry⁷. Kerr effect is one of the third order nonlinear optical effects with an induced nonlinear index which makes the refractive index to be defined as $n = n_0 + n_2 I$, where I is the intensity of laser beam. Besides Kerr effect, a cascaded second-order nonlinear optical effect called Kerr-like nonlinearity⁸ occurring in non-centrosymmetric crystals will induce a similar n_2 . Caumes et al⁹ have reported a THz waves related Kerr-like effect in ZnTe where femtosecond laser pulses generate THz waves via optical rectification and the generated THz waves modify the refractive index at optical frequency via electro-optic effect. A combination of the optical rectification and electro-optic effect induces an equivalent n_2 . It is necessary to distinguish Kerr and Kerr-like effect in LiNbO₃ because this kind of crystals has important applications in THz devices.

We present an optical pump-probe experiment on LiNbO₃. Unlike previous studies where only oscillations from phonon polaritons were investigated, we focus on the signals near

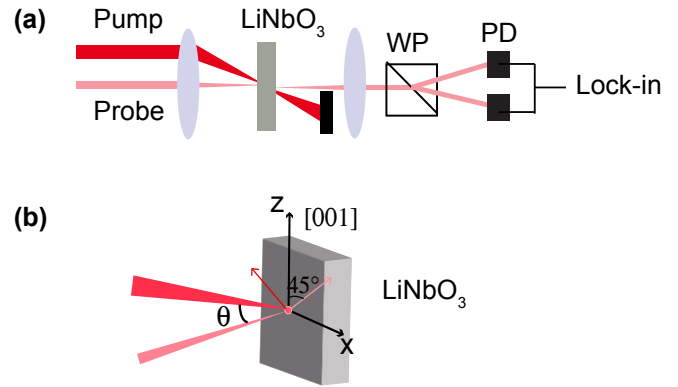


FIG. 1. (a) Pump probe experimental setup. (b) Geometries of sample and polarizations of the pump and probe beams.

zero-time delay. We demonstrate that both Kerr and Kerr-like effects contribute to this signal. Although a large velocity mismatch exists between laser pulses and THz waves in LiNbO₃, the obtained spectra still have obvious Kerr-like properties, which is inconsistent with previous results⁹ where only THz waves almost fulfilling the phase matching condition contribute obviously to n_2 .

Fig. 1 shows the setup for optical pump-probe experiment. A congruent MgO: LiNbO₃ (MgO 6%) wafer was used in our experiment. LiNbO₃ belongs to uniaxial crystals. Our sample was cut with its optic axis (defined as z axis) in the plane of surface (x-z plane) and its thickness of 2 mm. Both sides of our sample were polished. Femtosecond laser pulses generated by a commercial Ti:Sapphire oscillator with duration of 70 fs, repetition frequency of 80 MHz, central wavelength of 800 nm, were split into a pump beam and a probe beam. The pump beam, after being delayed by an optical stage and modulated by an optical chopper, was focused onto the surface of the LiNbO₃ wafer. The probe beam was focused at the same place as the pump beam, with the polarization per-

^{a)}Electronic mail: xiaojunwu@buaa.edu.cn

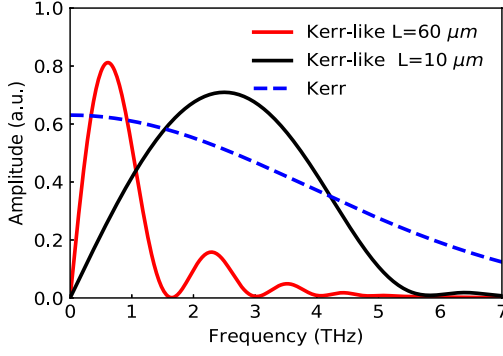


FIG. 2. Calculated pump probe spectra originated from Kerr (blue dash line) effect, Kerr-like effect when $L=60 \mu\text{m}$ (red line) and Kerr-like effect when $L=10 \mu\text{m}$ (black line).

pendicular to that of the pump beam to decrease the coherent spike signal¹⁰. The polarization of the probe beam was 45° off the optical axis, and the polarization variation induced by the pump beam was detected by a combination of a quarter wave-plate, a Wollaston prism and a balanced detector. The signal as a function of delay time was collected by a phase sensitive lock-in amplification technique. The pump beam was non-collinear with the probe beam. The average power of the pump beam was ~ 435 mW and that of the probe beam was ~ 20 mW. The spot size of the pump beam was larger than that of the probe beam. Before scanning the optical stage line, we blocked the pump beam and adjusted the quarter wave plate to make the output signal to be zero. We conducted all the experiments at the room temperature.

Firstly, we demonstrate theoretically that both Kerr and Kerr-like nonlinearities contribute to the pump-probe spectra. LiNbO_3 crystals at the room temperature belong to 3m point group¹¹ and their third order nonlinear susceptibility $\chi^{(3)}$ has 14 independent nonzero elements and, their second order nonlinear susceptibility $\chi^{(2)}$ has 4 independent nonzero elements¹². In our experiment, the pump beam induces a variation of dielectric tensor via $\chi^{(3)}$ given by

$$\Delta\epsilon^{Kerr} \propto \frac{1}{2} \begin{bmatrix} \chi_{xxxx} + \chi_{xxzz} & 2\chi_{xxzx} \\ 2\chi_{xxzx} & \chi_{zzxx} + \chi_{zzzz} \end{bmatrix} E^2, \quad (1)$$

where χ_{ijml} ($i, j, m, l = x, z$) is the component of $\chi^{(3)}$ and E is the electric field of the laser pulse. The induced $\Delta\epsilon^{Kerr}$ modifies the polarization of the probe beam. Since the $\chi^{(3)}$ effect here is instantaneous, for each time delay τ , the lock-in gives rise to a signal^{9,13}: $S^{Kerr}(\tau) \propto \int I^{pu}(t) I^{pr}(t - \tau) dt$, which is the correlation of the pump and probe beams, and has no negative part. The Fourier transform of $S^{Kerr}(\Omega)$ is shown in Fig. 2 (blue dash line). It is a descending function with a finite dc component.

The second order nonlinear susceptibility $\chi^{(2)}$ of LiNbO_3 contributes to the generation of THz electric fields via optical rectification of laser pulses, and the generated THz waves induce a modification of the dielectric tensor via electro-optic

effect. The sum effect gives rise to the Kerr-like effect and the induced change of the dielectric tensor is given by

$$\Delta\epsilon^{Kerr-like} \propto \frac{1}{2} \begin{bmatrix} \chi_{zxx}\chi_{zxx} & 2\chi_{zxx}\chi_{xxz} \\ 2\chi_{zxx}\chi_{xxz} & \chi_{zzz}\chi_{zzz} \end{bmatrix} E^2, \quad (2)$$

where χ_{ijm} ($i, j, m = x, z$) is the component of $\chi^{(2)}$. Here, the relations $\chi_{mij} = \chi_{mji}$ and $r_{ijm} \propto \chi_{mij}$ are involved, where r_{ijm} is the electro-optic coefficient. Eq. (2) means that $\Delta\epsilon_{ij}^{Kerr-like}$ can be induced with THz electric field E_m^{THz} via r_{ijm} , where the E_m^{THz} is generated by femtosecond laser pulses via χ_{mij} . The $\Delta\epsilon^{Kerr-like}$ has a similar form with the $\Delta\epsilon^{Kerr}$ and will also modify the polarization of the probe beam.

The generated THz wave has a propagation effect in LiNbO_3 . It is well known that there exists a large velocity mismatch between the laser pulses and THz waves in LiNbO_3 . The velocity mismatch will greatly influence both the generation and probe processes, which makes the spectrum shape of Kerr-like effect different from that of the Kerr effect. The spectrum due to the generation and detection of the THz waves is calculated according to Ref. 14. For the generation process, the THz electric field is expressed as

$$E(\Omega, z) = \frac{\mu_0 \Omega \chi_{eff}^{(2)} I(\Omega)}{in(\omega_o)[n(\Omega) + n_g]} \frac{e^{ik_0 n(\Omega)z} - e^{ik_0 n_g z}}{k_0 [n(\Omega) - n_g]}, \quad (3)$$

where $\chi_{eff}^{(2)}$ is the effective second order coefficient which is assumed as a constant; $n(\omega_o)$ and $n(\Omega)$ are the refractive index at optical frequency and THz frequency range, respectively; n_g is the group refractive index of laser pulses; z is position; $I(\Omega)$ is the spectrum of laser envelope; $k_0 = \Omega/c$, where c is the light velocity in vacuum. For the probe process, the spectrum of the signal obtained from the lock-in is described as

$$S^{Kerr-like}(\Omega, L) = k_0 \chi_{eff}^{(2)} I(\Omega) \frac{1 - e^{ik_0 [n(\Omega) - n_g]L}}{-i[n(\Omega) - n_g]} E(\Omega, L). \quad (4)$$

In the Ref. 14, L in Eq. (4) denotes the sample thickness. In our case, since the pump beam is non-collinear with the probe beam, L is defined as the interaction length, which can be controlled by the angle θ between the pump and probe beam as shown in Fig. 1.

To investigate the properties of the Kerr-like nonlinearity in the pump-probe experiment, we calculated the spectra when $L = 60 \mu\text{m}$ and $L = 10 \mu\text{m}$ according to Eq. (4). The parameters $n(\Omega)$ and $n(\omega_o)$ are given in Ref. 15. The calculated spectra $S^{Kerr-like}(\Omega)$ due to Kerr-like effect are also illustrated in Fig. 2. There exist two significant differences between spectra from the Kerr effect and the Kerr-like effect. First, $S^{Kerr}(0)$ has a finite value while $S^{Kerr-like}(0)$ vanishes. Second, $S^{Kerr-like}(\Omega)$ has an interference structure which is originated from the propagation of laser pulse and THz waves. The interference structure is dependent on the interaction length L . The smaller L makes a smaller structure. The whole spectrum $S(\Omega)$ is the sum of $S^{Kerr-like}(\Omega)$ and $S^{Kerr}(\Omega)$.

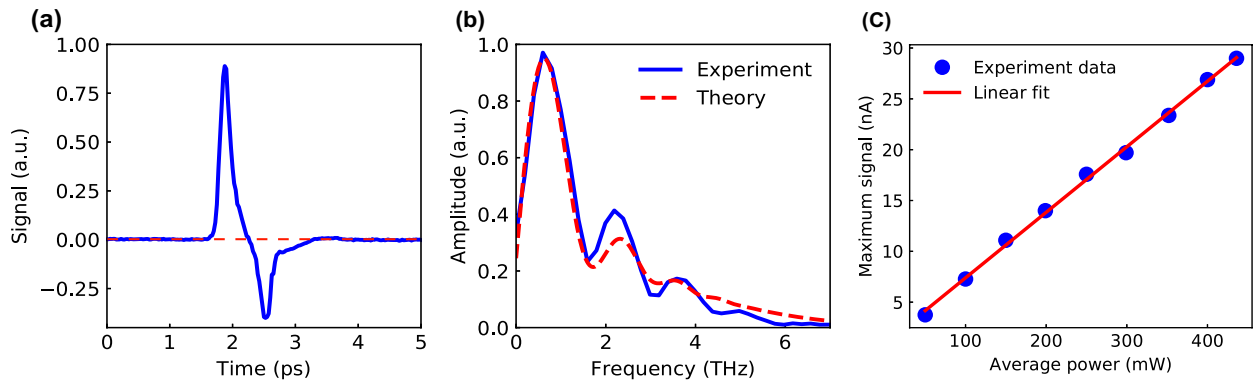


FIG. 3. (a) A typical waveform obtained from the pump-probe measurement. The red dash line is the guide line of zero signal. (b) The corresponding Fourier transform spectrum (blue line) and the calculated spectrum (red dash line). (c) Peak value of the waveform as a function of the pump power (blue circles) and the linear fit (red line) for the experimental data.

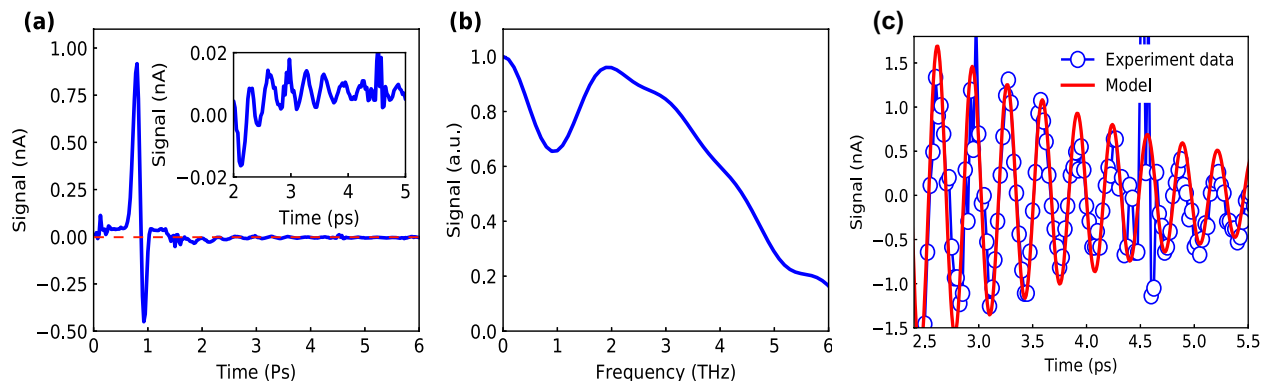


FIG. 4. (a) A pump-probe signal with a longer tail, and (b) its corresponding spectrum when the angle between the pump and the probe beams is $\sim 10^\circ$. Inset: the zoom in view of the oscillation waveform. (c) A damped oscillator model is employed to well fit the oscillatory waveform in 2-5 ps.

To evidence our theoretical analysis, we conducted pump-probe experiment at two different θ . A typical experimental signal recorded when $\theta \approx 5^\circ$ is depicted in Fig. 3(a). It has a one-cycle pulse with duration about 1.5 ps which has a negative part, indicating that THz related Kerr-like effect contributes to the signal. Fig. 3(b) shows the Fourier Transform spectrum of the waveform. This spectrum spans up to 6 THz and has an interference structure which is similar to that in Fig. 2.

According to our calculation, the interference structure originates from the large velocity mismatching between the THz waves and laser pulses. Besides, the spectrum has a nonzero dc component. These results indicate that both Kerr and Kerr-like nonlinearity play roles in n_2 . By adjusting the interaction length and the ratio between Kerr and Kerr-like spectra, we can reproduce the measured spectrum, as is shown in the red dash line in Fig. 3(b). We also conducted power dependent experiments. Fig. 3(c) shows the peak value of the waveforms as a function of the laser average power of pump beam. The line represents the linear fit of the experimental

data. It is obvious that the pump-probe signal scales linearly with the intensity, which is expected by both Kerr and Kerr-like nonlinearities.

We increased the angle between the pump beam and the probe beam to $\sim 10^\circ$ to decrease the interaction length. Figure 4(a) shows the waveform when the interaction length is decreased. There is a big one-cycle pulse followed by a small oscillation signal as shown in the inset. The duration of the main pulse is ~ 1 ps, which is a little smaller than that in Fig. 3(a). The Fourier transform spectrum of the main pulse is plotted in Fig. 4(b). It spans more than 6 THz, and the interference structure is not obvious. Besides, this spectrum has larger high frequency components than that shown in Fig. 3(b). These results are consistent with our calculation for the smaller interaction length.

Following the main pulse in Fig. 4(a), there is a long oscillation behavior. This is due to the coherent excitation of phonon polaritons. Pioneering works about coherent phonon polaritons excited by femtosecond laser pulses via impulsive Raman scattering have been reported by Bakker and Nelson

et al in Ref. 6 and 16. The oscillation is perfectly fitted by a damped harmonic oscillator function, seen in Fig. 4(c). The frequency of the phonon polaritons, obtained from the fitting of the experimental data, is ~ 3 THz, which is consistent with previous report¹⁷.

Even on a bad phase matching condition, we can still observe THz related Kerr-like nonlinearity when femtosecond laser pulses interacting with LiNbO₃. This observation is inconsistent with results reported by Caumes et al⁹. They did not observe an obvious Kerr-like nonlinearity contributing to n_2 due to the phase mismatch occurs in ZnSe. The reason for our results may be that $\chi^{(2)}$ of LiNbO₃ is larger than that of ZnSe. Distinguishing Kerr and Kerr-like nonlinearities is important because femtosecond laser pulses interacting with LiNbO₃ has important applications such as excitation and imaging of phonon polaritons.

Another aspect should be mentioned is that we only observed an obvious phonon-polariton signal when the interaction length is small. The reason is that phonon polaritons can propagate in the crystals. The phase mismatch also hinders the observation of phonon-polariton signal. When the interaction length is small, the phase mismatching effect is also small.

It is necessary to compare the THz related Kerr-like effect and intense THz wave induced Kerr effect. With the great development of intense THz sources, it becomes possible to observe third-order nonlinear effects in the THz frequency range. For example, Zalkovskij et al¹⁸ have observed THz-induced optical birefringence in amorphous chalcogenide glasses which are centrosymmetric. It is impossible to observe the THz related Kerr-like effect reported here in amorphous chalcogenide glasses because the $\chi^{(2)}$ of the centrosymmetric material vanishes. Besides, the Kerr-like effect in LiNbO₃ is non-instantaneous while the induced change of refractive index in amorphous chalcogenide glasses follows the intensity profile of the THz pulse.

In conclusion, we have conducted optical pump-probe experiments on LiNbO₃ with different angles between the pump beam and the probe beam. Both Kerr and Kerr-like nonlinear-

ities have been observed to contribute to n_2 with femtosecond laser pulses interacting with LiNbO₃. Besides, we also have excited and detected the low frequency phonon polaritons. Our experimental results agree well with theoretical analysis.

This work is supported by Beijing Natural Science Foundation (4194083), the National Natural Science Foundation of China (61775233, 11827807).

- ¹D. N. Nikogosyan, *Nonlinear Optical Crystals: A Complete Survey*, 2nd ed. (Cork, Ireland).
- ²O. Alibart, V. D'Auria, M. D. Micheli, F. Doutré, F. Kaiser, L. Labonté, T. Lughì, É. Picholle, and S. Tanzilli, *J. Opt.* **18**, 104001 (2016).
- ³E. L. Wooten, K. M. Kissa, A. Yi-Yan, E. J. Murphy, D. A. Lafaw, P. F. Hallemeier, D. Maack, D. V. Attanasio, D. J. Fritz, G. J. McBrien, and D. E. Bossi, *IEEE J. Sel. Top. Quantum Electron.* **6**, 69 (2000).
- ⁴H. A. Hafez, X. Chai, A. Ibrahim, S. Mondal, D. Férachou, X. Ropagnol, and T. Ozaki, *J. Opt.* **18**, 093004 (2016).
- ⁵J. Hebling, A. Stepanov, G. Almási, B. Bartal, and J. Kuhl, *Appl. Phys. B* **78**, 593 (2004).
- ⁶H. J. Bakker, S. Hunsche, and H. Kurz, *Rev. Mod. Phys.* **70**, 523 (1998).
- ⁷Y. R. Shen, *The principles of nonlinear optics* (New York).
- ⁸C. Bosshard, R. Spreiter, M. Zgonik, and P. Günter, *Phys. Rev. Lett.* **74**, 2816 (1995).
- ⁹J.-P. Caumes, L. Videau, C. Rouyer, and E. Freysz, *Phys. Rev. Lett.* **89**, 047401 (2002).
- ¹⁰C. W. Luo, Y. T. Wang, F. W. Chen, H. C. Shih, and T. Kobayashi, *Opt. Express* **17**, 11321 (2009).
- ¹¹R. S. Weis and T. K. Gaylord, *Appl. Phys. A* **37**, 191 (1985).
- ¹²R. Boyd, *Nonlinear Optics* (New York).
- ¹³Z. Tian, C. Wang, Q. Xing, J. Gu, Y. Li, M. He, L. Chai, Q. Wang, and W. Zhang, *Appl. Phys. Lett.* **92**, 041106 (2008).
- ¹⁴A. Schneider, M. Neis, M. Stillhart, B. Ruiz, R. U. A. Khan, and P. Günter, *J. Opt. Soc. Am. B* **23**, 1822 (2006).
- ¹⁵N. N. Zinov'ev, A. S. Nikoghosyan, R. A. Dudley, and J. M. Chamberlain, *Phys. Rev. B* **76**, 235114 (2007).
- ¹⁶T. P. Dougherty, G. P. Wiederrecht, and K. A. Nelson, *J. Opt. Soc. Am. B* **9**, 2179 (1992).
- ¹⁷B. S. Dastrup, J. R. Hall, and J. A. Johnson, *Appl. Phys. Lett.* **110**, 162901 (2017).
- ¹⁸M. Zalkovskij, A. C. Strikwerda, K. Iwaszczuk, A. Popescu, D. Savastru, R. Malureanu, A. V. Lavrinenko, and P. U. Jepsen, *Appl. Phys. Lett.* **103**, 221102 (2013).